熱帯熱マラリア原虫の培養系における増殖阻害アッセイ

岩永達也　加藤健太郎

東京大学 農学部 獣医微生物学研究室
〒113-8657　東京都文京区弥生 1-1-1

[抄録]　マラリアは、特に熱帯や亜熱帯地域で見られる感染症であり、アピコンプレクサ門に属するマラリア原虫の感染によって引き起こされる。既存の薬剤に対する耐性原虫の増加に伴い、原虫の感染・増殖を抑制する新規の薬剤・治療法の開発が急務となっている。本稿ではその研究開発の手法の一つとして、フラスコ内で培養した熱帯熱マラリア原虫に対する薬剤の増殖阻害効果を、血液塗抹の観察に依り定量的に検証する実験法について述べる。

キーワード；熱帯熱マラリア原虫、増殖阻害剤

Growth inhibition assay with *in vitro* culture of *Plasmodium falciparum*.

Tatsuya Iwanaga, Kentaro Kato

Department of Veterinary Microbiology, Faculty of Agriculture, The University of Tokyo
1-1-1 Yayoi, Bunkyo-ku, Tokyo 113-8657, Japan

Abstract: Malaria, which is caused by an Apicomplexan parasite, *Plasmodium* spp., is an infectious disease, especially seen in tropical and subtropical regions. Because of increasing resistant parasites to current medications, development of new drug or treatment which inhibits parasite infection and growth is needed. For this development activity, in this article, we described a method in which the effects of drugs on the culture of *Plasmodium falciparum* in flasks are measured quantitatively by microscopy of the blood smear.

Key Words: *Plasmodium falciparum*, growth inhibitor

[はじめに]

マラリアは、熱帯や亜熱帯地域で多く見られる人の感染症であり、ハマダラカの媒介によるアピコンプレクサ門に属するマラリア原虫の感染によって引き起こされる。アフリカでは特に感染者が多く、近年でも 100 万人近くの死者を出す未だ重大な疾病である。病原体となる原虫は中間宿主である人の血液に入ると、一旦肝細胞内で増殖するが、その後放出されるメロゾイトは赤血球内で増殖を繰り返す。治療は現在クロロキンやメフロキンの投与により行われるが、耐性原虫や副作用の問題のため、新しい薬剤・治療法の開発が求められている（Kato ら、2012）。本稿では、特に強い症状を引き起こすとされる熱帯熱マラリア原虫をフラスコ内で培養し、そこへ薬剤を投与することによって現れる増殖阻害効果を、血液塗抹を顕微鏡観察することにより評価する方法について述べる。

[方法]

1. 使用する原虫株と宿主細胞、試薬類

マラリア原虫として、熱帯熱マラリア原虫 HB3 株を使用した。宿主として、AB 型人血液（採血から 2 週間以内）を用いた。血液塗抹の染色にはライト・ギムザ染色を用いた。また、原虫のライフサイクルの同調にヘパリンナトリウム水溶液、5%D-ソルビトール水溶液を使用した。

2. 薬剤添加による増殖阻害アッセイ

熱帯熱マラリア原虫の赤血球内増殖期は、赤血球侵入後 20 時間までに見られるリング期、その後見られるトロホゾイト期（侵入後 20 時間～36 時間）、核の分裂が観察できるシゾント期（侵入後 36 時間～44 時間）の 3 期に分けられる。

原虫の培養におけるライフサイクルを同調させるため、ヘパリンによる侵入阻害効果を利用する。原虫の培養液中に最終濃度 30 単位/ml となるようにヘパリンナトリウム水溶液を加え、44 時間培養する。44 時間後、培養液中の赤血球を新しい液体培地で洗浄し、4 時間インキュベートすることにより、この間原虫は新しい赤血球に侵入することができる。培養液を遠心分離して上清を捨てた後、赤血球体積の 9~10 倍量の 5%D-ソルビトール水溶液を加えて激しく振盪して後期トロホゾイト・シゾント期の原虫を死滅させる。再び赤血球を液体培地で洗浄するすると、培養液中にはヘパリンを洗浄してから 4 時間の間に新たに赤血球に侵入したリング期の原虫だけが残る。この方法により、理論上 4 時間の幅で原虫のライフサイクルを同調させることができる。

原虫の培養液を新しい液体培地とともに 96 ウェルプレート（U 底）に分注する。ヘマトクリット（培養液に対する赤血球の体積比率）は

1%、パラシテミア（全赤血球数に対する感染赤血球数比率）は 0.5%程度が望ましい。今回は原虫がトロホゾイト期にあるときに薬剤とともに分注し、48 時間の培養を開始した。あらかじめプレートに2倍濃度の薬剤の入った液体培地を入れておき、そこへヘマトクリット2%の培養液同量を一斉に加えると、実験の開始がスムーズに行える。対照実験には、薬剤の溶媒を同じ濃度となるように加えたものを用いる。

48 時間の培養により、マラリア原虫のライフサイクルが一周する。各ウェルから上清を取り除き、各々の培養液で血液塗抹を作製する。ライト・ギムザ染色により血液塗抹を染色し、顕微鏡で観察する。全赤血球 10000 個に対する感染赤血球の個数を数え、その割合を算出する。薬剤の入っていない対照実験の培養液では、2.5~3%となることが見込まれる。対照実験に対する各薬剤・各濃度で得られた感染率の割合を評価することにより、それらの薬剤の増殖阻害効果を見ることができる。

[結果]

薬剤の入っていない対照実験に対するパラシテミアの減少の度合いから、その薬剤の原虫に対する増殖阻害効果を検証することができる（図）。また、薬剤濃度を段階的に設定することにより、薬剤効果の濃度依存性を調査することもでき、対照の 50%のパラシテミアを示した薬剤濃度をその薬剤の IC_{50} 濃度とすることができる。

マラリア原虫はシゾント期を経た後、宿主細胞を破って培養液中に出、新たな赤血球に侵入する。したがって、シゾント期～リング期間は原虫数が増加する移行期となる。リング期から実験を開始し、次のリング期でサンプル回収とすると、薬剤の効果等によりまだ一部の原虫が移行期にある場合に感染率が安定せず正確に評価することができない。トロホゾイト期に実験を開始し次のトロホゾイト期で回収することにより、感染率が不安定になるのを抑え、なおかつ薬剤がどこかの段階で増殖に影響を与えていればその影響を感染率の変化として検出できる。

[考察]

96 ウェルプレートを用いて、それぞれの条件下において熱帯熱マラリア原虫を培養することにより、原虫の増殖具合から薬剤の原虫増殖に対する影響を評価することができる。マラリア原虫の培養には本来細かな頻度での液体培地の交換が必要となるが、ヘマトクリット値・パラシテミアをともに低値に設定することによりそれを必要とせず、加える薬剤の濃度以外の条件をそろえて実験を行うことができる。

ここで述べた実験方法を用いることで、投与した薬剤により原虫のリング期からトロホゾイト期への遷移やシゾント期の核分裂、新しい宿主細胞への侵入など、赤血球内サイクルのどこかが抑制されていれば、それらを原虫の増殖阻害効果として検出することができる。この実験方法だけでは、どの部分を薬剤が抑制しているかまでは判断できないが、原虫のライフサイクルの同調がうまくいっていれば、薬剤の投与とサンプル回収のタイミングを変えることによりそれらを推測することができる。

また、一つのウェルに入れる原虫培養液の量を増やしたり、ウェルの数を増やしたりすることにより、薬剤を投与してからの原虫発育の経時的変化を観察することもできる。しかしその場合、原虫を培養するインキュベーターからプレートを外へ出す回数が増えることにより原虫の発育が遅れてしまい、実験結果に影響を及ぼす可能性があるため注意が必要である。

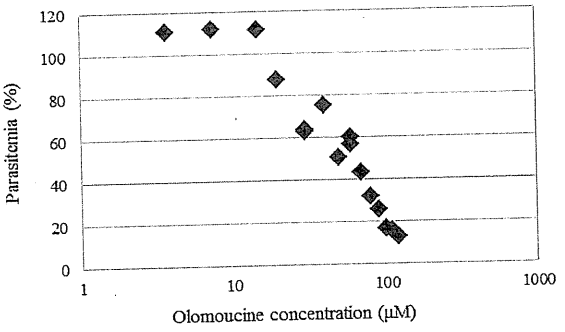

図：薬剤として Olomoucine(Calbiochem)を使用した例。x 軸に薬剤の濃度、y 軸に対照実験に対するパラシテミアの比率をとった。

[謝辞]

本研究は、科学研究費補助金・若手研究、生物系特定産業技術研究支援センター・イノベーション創出基礎的研究推進事業により行われた。

[文献]

1) Kato K, Sugi T, Iwanaga T.: Roles of Apicomplexan protein kinases at each life cycle stage. Parasitol Int. 61:224-234, 2012

トキソプラズマ原虫の培養と精製

杉　達紀　加藤健太郎

東京大学大学院農学生命科学研究科獣医微生物学研究室
〒113-8657　東京都文京区弥生 1-1-1

[抄録] ここではトキソプラズマ原虫を使用した実験系に必須となるトキソプラズマ原虫の培養増殖及び、単離方法について手順をおって紹介する。

キーワード；トキソプラズマ原虫、哺乳類培養細胞、精製法

In vitro culture of *Toxoplasma gondii* with mammalian cells as hosts

Tatsuki Sugi, Kentaro Kato

Department of Veterinary Microbiology, Graduate School of Agricultural and Life Sciences,
The University of Tokyo
1-1-1 Yayoi, Bunkyo-ku, Tokyo 113-8657, Japan

Abstract: Here the authors report the step-by-step way to culture, propagate and purify *Toxoplasma gondii* parasite. Purification of parasites is the first step of all experiments using *Toxoplasma gondii*.

Key Words: *Toxoplasma gondii*, *in vitro* culture, purification

---

[はじめに]

トキソプラズマ原虫は再興感染症の病原体であることからも、マラリア原虫と同じ門に属し、かつ遺伝子操作などが容易であることからも、原虫の実験材料としては非常に適している。ここでは、宿主細胞として哺乳類の細胞を用いてフラスコ内でトキソプラズマ原虫を大量に培養する方法及び、生きたトキソプラズマ原虫を精製する方法を、成書（Striepen ら、2007）に本研究室で加えた変更点を踏まえ、MOI、培地、取り扱い操作などの詳細を紹介したい。

[方法]

我々は、トキソプラズマ原虫の宿主細胞としてウイルス等の宿主細胞を必要とする病原体の増殖によく用いられている Vero 細胞を利用している。以下は Vero 細胞を宿主細胞とした場合の培地組成などを紹介する。

[A] 材料、道具

【細胞】

Vero 細胞
（Riken Bio Resource Center: RCB0001）

Toxoplasma gondii
（ATCC から各種系統が入手可能）

ToxoDB (http://www.toxodb.org/) には入手可能なトキソプラズマ原虫のゲノムプロジェクトのデータがまとまっており、ゲノム情報が利用可能な株を確認することができる。

【培地】

DMEM (Dulbecco Modified Eagles' medium) (Nissui #05919)
5%FCS 添加 DMEM（Vero 細胞培養用）
1%FCS 添加 DMEM（感染細胞培地用）
10%DMSO 添加 FCS（凍結保存液）

[B] 培養の実際

（１）哺乳類宿主細胞の用意

トキソプラズマ原虫は偏性細胞内寄生生物であるため、宿主細胞が培養には必須である。フラスコを最大限利用するためには、宿主細胞はフラスコの底面全面に confluent で培養されている状態が好ましい。トキソプラズマ原虫接種日の前夜に confluent の Vero 細胞を 3:1 で希釈して播種したフラスコを用意することで、安定して confluent の Vero 細胞を用意することができる。

（２）凍結トキソプラズマ原虫の接種

ATCC などより入手したトキソプラズマ原虫は凍結状態であるので、培地で洗浄後フラスコ内の宿主細胞に接種する。

i) 凍結バイアルを３７℃で速やかに融解する。
ii) 10 倍量（10ml 程度)の感染培地で希釈し 2000rpm, 5 分, 4℃での遠心を行う。
iii) 上清を除き、感染細胞用培地 5ml にピペッティングで優しく懸濁する。
iv) 接種先の Vero 細胞フラスコから増殖培地を除く。
v) 原虫懸濁液を Vero 細胞フラスコに接種する。この時フラスコの蓋は密栓しない。
vi) 37℃, 5%CO_2 の通常の哺乳類細胞培養条件で 30 分ほど静置する（フラスコ内の CO_2 濃度を平衡化するため）。
vii) 一度インキュベータから取り出し、蓋を密栓する。万が一の場合にトキソプラズマ原虫の

汚染が広がらないようにするためと、外からのコンタミを防ぐためである。Vero 細胞が confluent であるため、はじめに CO_2 濃度の平衡化をすれば密栓した状態でも原虫は元気に増殖する。
viii) 原虫の増殖が顕微鏡下で確認できるまで、2日毎に感染細胞用培地を交換し、培養を続ける。

（3）トキソプラズマ原虫の精製、継代
原虫の姿が顕微鏡下で確認できたら（図1、コロニーの様子）、原虫の精製および継代を行う。継代先の Vero 細胞は（1）の項と同様に用意しておく。

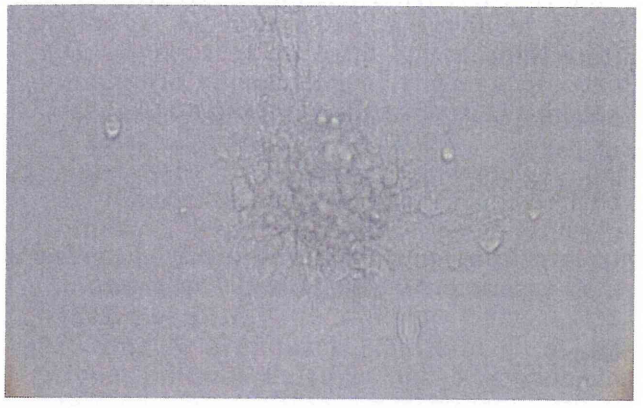

図1．20×10 倍で観察した原虫増殖箇所

準備する器具
5ml シリンジ（培養スケールによって変更する）
25G 針
径 5um フィルター
（我々は、シリンジに直接付けられる Millipore 社の Millex SV 5.00um を利用している。）
スクレーパー

i) スクレーパーで感染細胞を剥がす（図2）。

図2．スクレーパーを用いた感染細胞の回収

ii) 5ml シリンジと 25G 針を用いて宿主細胞を破壊する（図3）。2～3回出し入れし、最後にシリンジに吸い込んでおく。針の先を折るとフラスコの端にアクセスしやすい。

図3．シリンジと中折れ針による感染細胞の破壊操作

iii) シリンジから針を外し、5um フィルターを取り付け、感染細胞懸濁液をフィルターでろ過し遠心管に回収する（図4）。この時、5um より小さい原虫細胞と破壊された宿主細胞塊はフィルターを通るが、5um より大きい Vero 細胞は通らないので原虫のみを回収することができる。

図4．シリンジに取り付けたフィルターでの原虫濾過

iv) 濾過した原虫懸濁液を、2000rpm, 10分, 室温で遠心し、原虫を回収する。
注）トキソプラズマ原虫を低温、37℃などで繰り返し温度変化させると、原虫の生存率が下がる報告がある（Carruthers ら、1999）ことから（原虫の侵入に関わる分泌機能が失われる）我々は精製の操作中は常に室温で扱うことにしている。
v) 上清を除き感染培地もしくは PBS などのバッファーを 5ml 加え原虫を懸濁する。
vi) iv)～v)をさらに2回繰り返し原虫を洗浄する。
vii) 原虫を 5ml の感染培地もしくは目的とするバッファーに再懸濁し、顕微鏡下で計数する。我々は一般的な血球計算盤を用いて対物 20 倍、対眼 10 倍の倍率を用いている。（図5）。

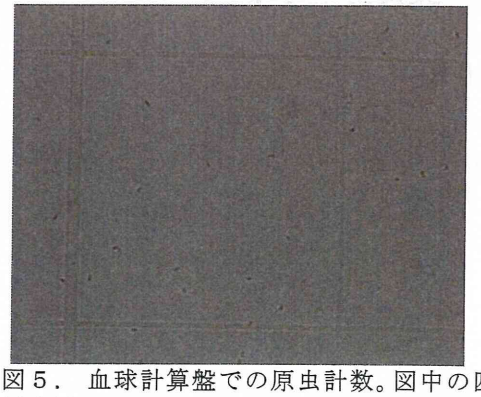

図5．血球計算盤での原虫計数。図中の四角の一片の長さは 0.025mm。

トキソプラズマ原虫は三日月型をした細胞として観察される。

viii) multiple of infection (MOI)が 0.1 から 1 になるように感染培地 5ml に原虫を希釈し、増殖培地を除いた Vero 細胞フラスコに接種する。

ix) MOI が 1 の場合は 24 時間程、MOI が 0.1 の場合は 48 時間ほどで宿主細胞が全て原虫に破壊され（図 6）、次回の原虫の継代や原虫の精製回収に使用できるようになる。時間についてはトキソプラズマ原虫の系統株によるものもあるので、事前に MOI を振り条件検討をしておくとよい。

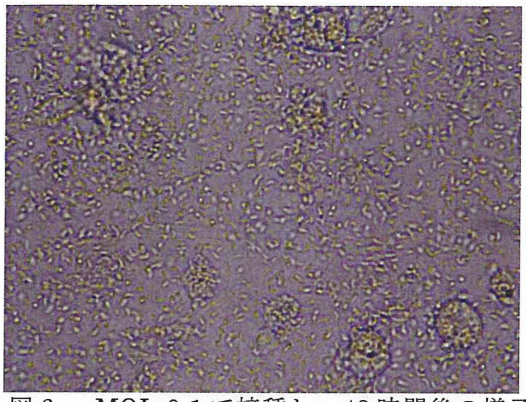

図 6． MOI=0.1 で接種し、48 時間後の様子

注 1) 材料として原虫を用いる場合には、i)-vii)までの手順に従うが、MOI を管理して接種した感染細胞から回収した原虫の方が、原虫数や生存率などが揃ったいきの良い原虫を得られる。

注 2) MOI を管理したい場合には継代時に原虫の精製をする必要があるが、継代後に原虫サンプルを回収する必要などなく、単純に継代をしたい場合には、手順 i)のスクレーパーによる剥離後にピペッティングで懸濁し、10 分の 1 量を次の Vero 細胞に接種すれば良い。

（4）凍結保存方法

培養を一時中止したい時や、原虫材料を送付するときなどに凍結保存が有効である。培養細胞全般と同じ方法で凍結サンプルを作成することができる。我々は感染細胞ごと凍結する方法で問題なく保存できている。

i)（3）の方法に従って原虫を継代後、感染細胞が破壊される 24 時間程前に（例えば、MOI を 0.1 で接種した場合は 24 時間の培養時間で）回収を行う。

ii) 感染細胞をスクレーパーでフラスコから剥がし、ピペットで遠心管に回収する。

iii) 1000rpm, 4℃, 5 分間の遠心を行い、上清を除く。

iv)凍結保存液に再懸濁し（T25 の感染細胞を 2ml に懸濁し、2 本のバイアルという計算で凍結している）、凍結用バイアルにいれ、プログラムフリーザーや BICELL などの器具を用いて-80℃にて冷凍する。

v) 凍結した細胞は液体窒素に保管し、半永久的に保存が可能である。

（5）クローニング

遺伝子組み換えや、突然変異、自然変異などで新たな性質を持った原虫を作出した場合、クローニングをすることで原虫株の樹立が行える。我々は、96well プレートを用いた限界希釈法でクローン化を行なっている。

準備する器具

□96well プレートに（1）と同様に 3 : 1（およそ 1.0×10^4 細胞/well）の希釈度で Vero 細胞を播種し一晩培養したもの。

□クローニングしたい原虫を含む原虫群

i) 2 倍階段希釈をするために、96well プレートに培養した Vero 細胞から培地を取り除き、感染培地 100ul を全 well へ加える。

ii)（3）の手順に従い、クローニングをしたい原虫群感染細胞から原虫の精製を行い、原虫数が 2.0×10^3/ml となるように感染細胞用培地で希釈する。

iii) 96well プレートの 1A から 1H までの 8well に原虫希釈液を 100ul ずつ加え、8 連のマルチピペッターなどを用いて、5 回混合し 100ul をとり 2A-2H の well に加える。

iv) 同様に混合した後に 100ul ずつ隣の Well へ加えて、11A-11H の列まで 2 倍階段希釈を続ける。

v) 11A-11H で混合した 100ul の原虫希釈液は廃棄し、接種されたプレートを用意する。

vi) 一週間程 37℃, 5%, CO_2 で培養し、顕微鏡下で 1 つのコロニー/well で観察される well を選択する。（5 日目ほどから観察できるようになるが、培養中にプレートに振動を与えるとコロニーが分散して一つの原虫由来のコロニーかどうかの判別が難しくなるので注意を要する）

vii) 各列でコロニー陽性 Well 率が 50%以下となっている希釈列から数個の well を選択し継代に用いる。（接種後 7 日目～8 日目）

viii) 継代日の前日に Vero 細胞を 24well プレートに用意する。

ix) 継代する well をマイクロピペットで勢いよくピペッティングし、（10 回ほど）、顕微鏡下で感染細胞と宿主細胞が well の底から離れていることを確認する。

x) 感染細胞懸濁液を 24well プレートの well に接種する

xi) その後感染細胞が破壊されるタイミングで、順に 6well プレート, T25 フラスコへと継代する。

[結果]

MOI 0.1 で摂取し、4 8 時間後に感染細胞の破壊を確認した（図 6）。

T75 フラスコから、1.0×10^9 のタキゾイトを得ることができた。

[考察]

一般的な成書では HFF 細胞を宿主細胞とし

て使っており、その入手面や維持のしやすさを考えるとVero細胞でのトキソプラズマ培養は研究室に導入しやすい。また、室温での操作を徹底することで、37℃に繰り返し暴露されることによって活性を失う（Carruthersら、1999）ことのない元気なトキソプラズマ原虫を得られ、後のアッセイにとって再現性のある良い材料をえることができる。

また、MOIを管理することにより宿主細胞の破壊産物が少ない状態でトキソプラズマ原虫培養液を得ることができる。これにより、原虫精製後の純度と収量を上げることが可能となる。

限界希釈法において、やや高めの希釈度から希釈列を作ることにより、効率的にクローンを得ることができる（Sugiら、2010）。

[謝辞]
本研究は、文部科学省特別研究奨励費及び科学研究費補助金・若手研究、生物系特定産業技術研究支援センター・イノベーション創出基礎的研究推進事業により行われた。

[文献]
1) Striepen B, Soldati D.: Genetic Manipulation of *Toxoplasma gondii*. *Toxoplasma gondii* The Model Apicomplexan: Perspectives and Methods, Elsevier, UK, 2007、p392-418.
2) Carruthers VB, Giddings OK, Sibley LD.: Secretion of micronemal proteins is associated with *Toxoplasma* invasion of host cells. Cell Microbiol, 1:225-35, 1999.
3) Sugi T, Kato K, Kobayashi K, et al.: Use of the kinase inhibitor analog 1NM-PP1 reveals a role for *Toxoplasma gondii* CDPK1 in the invasion step. Eukaryotic Cell, 9:667-70, 2010.

Arch Virol (2013) 158:1003–1011
DOI 10.1007/s00705-012-1577-3

ORIGINAL ARTICLE

Attenuation of an influenza A virus due to alteration of its hemagglutinin-neuraminidase functional balance in mice

Fumihiro Gen · Shinya Yamada · Kentaro Kato · Hiroomi Akashi · Yoshihiro Kawaoka · Taisuke Horimoto

Received: 5 October 2012 / Accepted: 9 November 2012 / Published online: 18 December 2012

Abstract Influenza A viruses possess two surface glycoproteins, hemagglutinin (HA), which binds to sialic-acid-containing receptors, and neuraminidase (NA), which removes sialic acid from host cells. It is well established that the HA-NA functional balance regulates the efficiency of virus replication. Here, we selected a plaque variant of the WSN (H1N1) strain that grew better than the wild-type virus in NA-expressing MDCK cell culture. A reverse genetics study revealed that the single mutation HA E190K, which occurs infrequently in naturally isolated H1N1 viruses, was responsible for the phenotype of this variant. Receptor assays indicated that this mutation did not affect the receptor specificity of HA but enhanced its receptor-binding affinity, resulting in altered HA-NA functional balance relative to that of the wild-type virus. We also found that this variant replicated in nasal turbinates at an equivalent level but in lungs at a lower level compared with wild-type virus, demonstrating its attenuation in mice. Together, our data demonstrated the importance of the HA-NA functional balance for influenza virus replication in an *in vivo* biological setting.

F. Gen · K. Kato · H. Akashi · T. Horimoto (✉)
Department of Veterinary Microbiology,
Graduate School of Agricultural and Life Sciences,
The University of Tokyo, Tokyo 113-8657, Japan
e-mail: ahorimo@mail.ecc.u-tokyo.ac.jp

S. Yamada · Y. Kawaoka
Division of Virology, Department of Microbiology
and Immunology, Institute of Medical Science,
The University of Tokyo, Tokyo 108-8639, Japan

Y. Kawaoka
ERATO Infection-Induced Host Responses Project,
Saitama 332-0012, Japan

Y. Kawaoka
Department of Pathobiological Sciences, School of Veterinary
Medicine, University of Wisconsin-Madison,
Madison, WI 53706, USA

Y. Kawaoka
International Research Center for Infectious Diseases,
Institute of Medical Science, The University of Tokyo,
Tokyo 108-8639, Japan

Introduction

Influenza A viruses are enveloped viruses that contain a segmented genome of eight different negative-strand RNA molecules. The envelope carries two surface glycoproteins, hemagglutinin (HA) and neuraminidase (NA). Both glycoproteins recognize the same host-cell molecule, sialic acid. HA binds to sialic-acid-containing receptors on target cells to initiate virus infection, whereas NA cleaves sialic acids from cell receptors to facilitate progeny virus release from cells. NA also cleaves extracellular mucus inhibitors containing sialic acids and prevents HA-mediated self-aggregation of virions by desialylation of virus glycoconjugates, promoting the spread of the infection to neighboring cells [3].

It is well established that the interplay between HA receptor-binding and NA receptor-destroying activities affects virus replication in eggs and cell culture; an optimal HA-NA functional balance is required for efficient virus replication [18]. In addition, a recent study showed that the HA-NA functional balance is critical for efficient respiratory droplet transmission of a pandemic H1N1 virus in ferrets, thereby contributing, at least in part, to virus pathogenicity in host animals [20]. Functional imbalance between HA and NA could be caused by mutations around the HA receptor-binding site, the NA enzymatic active site

or both, under various selective pressures of *in vitro* and *in vivo* biological environments [5, 6, 13, 19].

Here, we selected a plaque variant of the influenza A virus laboratory strain WSN (H1N1) in cell culture stably expressing viral NA and found that its HA-NA functional balance differed from that of the wild-type WSN virus, leading to a change in its plaque phenotype and growth properties in cell culture. To gain further insight into the responsibility of the HA-NA functional balance for the virus phenotype, we performed *in vivo* experiments showing that this variant exhibited reduced pathogenicity in mice.

Materials and methods

Cells and virus

Madin-Darby canine kidney (MDCK) and human embryonic kidney 293T cells were maintained in minimal essential medium (MEM) supplemented with 5 % newborn calf serum (NCS) and in Dulbecco's modified Eagle's medium with 10 % fetal calf serum, respectively. Cells were maintained at 37 °C in 5 % CO_2. We used A/WSN/33(H1N1; WSN) virus maintained in our laboratory. The WSN virus was propagated in MDCK cells in serum-free medium with 0.3 % bovine serum albumin (BSA) and 1 μg/ml TPCK-trypsin and was stored at −80 °C until use.

Reverse genetics

To generate a WSN mutant, we used our previously produced series of PolI constructs, derived from the WSN strain, for plasmid-based reverse genetics [15]. We also used pCAGGS plasmids expressing WSN NP, PA, PB1, or PB2 under the control of the chicken β-actin promoter for the system. Briefly, PolI plasmids generating viral RNAs and protein expression plasmids were mixed with a transfection reagent, Trans-IT 293T (Panvera), incubated at room temperature for 15 min, and then added to 293T cells. Transfected cells were incubated in Opti-MEM I (GIBCO-BRL) for 48 h. Supernatants containing infectious viruses were harvested, biologically cloned by limiting dilution in MDCK cells, and used for further experiments.

Cells stably expressing NA

MDCK cells were co-transfected with plasmids expressing WSN NA (pCAGGS-NA) and puromycin N-acetyltransferase, using an electroporator (Amaxa) according to the manufacturer's instructions. A cell clone that stably expressed NA was then selected in MEM containing 5 % NCS and puromycin dihydrochloride (5 μg/ml). NA expression was confirmed by immunostaining with an anti-NA mouse monoclonal antibody (WS5-29; a gift from Dr. Takashita, Yamagata University, Japan) after confluent cells were washed with phosphate-buffered saline (PBS) and fixed with 4 % paraformaldehyde in PBS for 30 min at room temperature. NA enzyme activity of the cells was measured using a commercial assay kit with fluorescent methylumbelliferone N-acetylneuraminic acid (MUNAN-A) substrate (NA-Fluor™ kit; Applied Biosystems).

Viral replication in cell culture

The plaque assay was conducted with MDCK cells and TPCK-trypsin (1 μg/ml). The growth kinetics of viruses was assessed in MDCK cells inoculated at a multiplicity of infection (MOI) of 0.01 PFU/cell. After adsorption for 1 h, the cells were overlaid with MEM containing 0.3 % BSA and TPCK-trypsin and were incubated at 37 °C. At various times post-infection, virus titers in the culture supernatant were determined using plaque assays.

Receptor-specificity analysis with sialylglycopolymers

Glycopolymers composed of poly-α-L-glutamic acid backbones with 5-*N*-acetylneuraminic acid linked to galactose through either α2,3 or α2,6 bonds (Neu5Acα2-3LacNAcb-pAP and Neu5Acα2-6LacNAcb-pAP) were chemoenzymatically synthesized as described elsewhere [17]. Virus suspension (200 HA units/ml) diluted in ice-cold PBS was used to coat 96-well polystyrene microplates (F96 Cert. MaxiSorp Nunc-Immuno Plate; Nunc), which were then incubated for 5 h at 4 °C (on ice). As a control, wells without virus were also incubated. Unbound virus was removed by washing the wells three times with ice-cold PBS. The wells were then blocked by incubating them at 4 °C overnight with 300 μl of PBS containing 0.001 % Tween 20 (TPBS). The virus-coated wells were then washed three more times with ice-cold PBS before 25 μl of horseradish peroxidase (HRP)-conjugated bovine fetuin (which possesses both Neu5Acα2-3Gal and Neu5Acα2-6Gal) diluted in TPBS (1:2,000) was added. Then, 25 μl of serially diluted sialylglycoconjugated polymers was added, and the plates were incubated at 4 °C for 2 h. After being washed five times with ice-cold PBS, the plates were incubated with 100 μl of substrate solution (0.4 mg/ml of *o*-phenylenediamine, 0.01 % H_2O_2 in 50 mM citrate-phosphate buffer, pH 5.5) at room temperature for 10 to 20 min. To stop the reaction, 50 μl of 0.1 N H_2SO_4 was added to each well. The extent of inhibition of fetuin binding to virions with sialylglycoconjugate polymers was determined by measuring the absorbance at 490 nm.

Virus elution assay from erythrocytes

Fifty μl of a twofold dilution of virus with an HA titer of 1:64 was incubated with 50 μl of 0.5 % chicken or 0.8 % guinea pig erythrocytes in a microtiter plate at 4 °C for 1 h. The plate was then stored at 37 °C, and the reduction in HA titer was recorded periodically. Opti-MEM was used as a diluent.

Viral pathogenicity in mice

Five-week-old female BALB/c mice (n = 10/group) were infected intranasally with 50 μl of viral suspension containing diluted viruses in sterile 0.9 % sodium chloride. Animals (n = 4/group) were monitored daily for survival over the next 14 days. On days 3 and 6 post-inoculation, three mice per group were euthanized, and their lungs, trachea, and nasal turbinates were harvested and titrated for the presence of virus.

Vaccine studies

Five-week-old female BALB/c mice (n = 4/group) were infected intranasally with the variant virus; control mice (n = 4) were inoculated with PBS. At day 22 post-vaccination (challenge day), all of the mice were similarly infected with 100 median mouse lethal doses (MLD_{50}) of wild-type WSN virus. Survival was monitored daily for the next 14 days.

Results

Establishment of cells stably expressing NA

Previous reports indicated that mutant viruses with an altered HA-NA functional balance could be obtained by using MDCK cells that had been treated with exogenous bacterial NA or lectin [5, 6]. Here, we established NA-expressing cells to obtain such a virus, and selected a cell clone designated as NA-MDCK cells. Immunostaining with an anti-NA antibody confirmed NA expression on the cell surface, although the reactivity appeared to be weak (Fig. 1a), possibly suggesting a low level of NA expression. Therefore, we performed fluorescent-activated cell sorting (FACS) analysis with the anti-NA antibody, which clearly showed that the NA-MDCK cells expressed NA on their surface (Fig. 1b). To assess the enzyme activity of NA expressed on cell surface, we used an MUNANA-based assay, which showed positive NA activity of NA-MDCK cells with cell numbers of more than 2.5×10^3, unlike MDCK cells.

To confirm that the expressed NA was functional, we used FACS analysis with two lectins, MALII, which is specific for sialic-acid-linked galactose with an α2,3 linkage (SAα2,3Gal), and SNA, which is specific for sialic-acid-linked galactose with an α2,6 linkage (SAα2,6Gal). The assay demonstrated that the parent MDCK cells possessed both types of SA, as reported previously [8]. By contrast, NA-MDCK cells retained strong binding to MALII lectin but showed weaker SNA lectin binding than that of the MDCK parent (Fig. 1c), indicating a reduction in the amount of SAα2,6Gal at the cell surface. This observation suggests that WSN NA, when expressed on the cell surface, cleaves SAα2,6Gal but not SAα2,3Gal.

Selection of plaque variants on NA-expressing cells

We next infected NA-MDCK and parental MDCK cells with WSN virus. Inoculation with a 10^{-4} dilution of the virus stock produced no visible plaques on NA-MDCK cells, whereas large plaques were clearly observed on the MDCK parent cells (Fig. 2). However, inoculation with a 10^{-2} dilution of virus produced large plaques on NA-MDCK cells, whereas on the MDCK parent, all of the cells were damaged by cytopathic effects (data not shown). Of note, many pinpoint plaques, which were not clearly detected by staining with crystal violet, were also present around the large plaques on NA-MDCK cells. These data indicate that WSN virus forms pinpoint plaques on NA-MDCK cells and that the viruses forming large plaques on this cell clone are probably variants. To further analyze the plaque variants, we purified them by three plaque-to-plaque passages on NA-MDCK cells and designated them as WSN-LPv.

A mutation determines the plaque phenotype of the variant

We hypothesized that the HA-NA functional balance of the WSN-LPv variant differed from that of parent WSN and that it matched the receptor properties or distribution on NA-MDCK cells. To test this concept at the molecular level, we examined the HA and NA gene sequences of WSN-LPv and found only one amino acid difference at position 190 (H3 numbering) of the HA; the parent WSN HA possessed Glu (E), whereas the variant HA possessed Lys (K). We observed no differences between amino acid sequences of the two NAs.

To determine the role of this HA E190K mutation in the large-plaque phenotype on NA-MDCK cells, we used reverse genetics to generate a mutant WSN virus with the HA E190K substitution, which was designated the WSN-E190K(HA) virus. We found that this virus formed large plagues on NA-MDCK cells, as did WSN-LPv (Fig. 3),

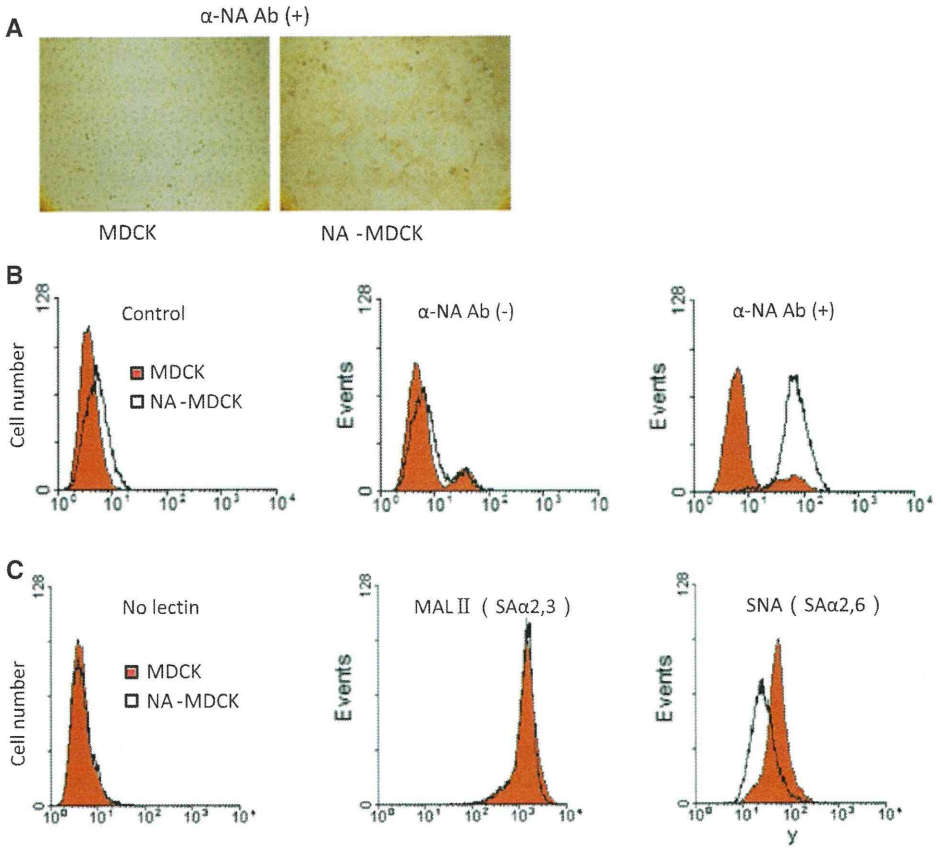

Fig. 1 Characterization of NA-expressing MDCK cells (NA-MDCK). **a** Immunostaining with an anti-NA antibody (α-NA Ab). A commercial ABC kit (Vector Laboratories) was used for detection. **b** FACS analysis of NA expression on the MDCK and NA-MDCK cell surface. An anti-mouse IgG FITC conjugate was used as the secondary antibody. **c** FACS analysis of the sialic acid content on the MDCK and NA-MDCK cell surface. MALII lectin, specific for SAα2,3Gal, and SNA lectin, specific for SAα2,6Gal, were used for the analysis

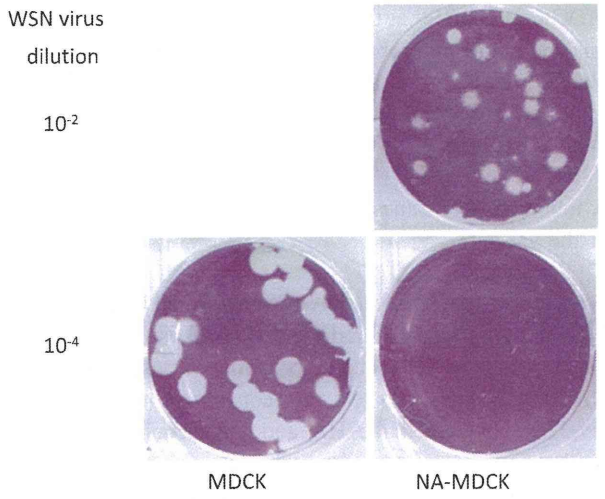

Fig. 2 Plaque morphology of the parent WSN virus on MDCK and NA-MDCK cells. Crystal violet staining was used to visualize plaques 2 days post-infection. All MDCK cells were detached from the well surface due to the cytopathic effect of the WSN virus at a dilution of 10^{-2} (not shown)

demonstrating that the single mutation of E190K in HA is responsible for the large-plaque phenotype of WSN-LPv on NA-MDCK cells.

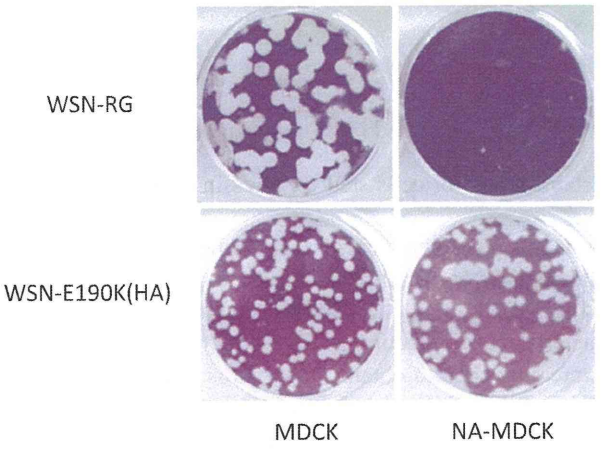

Fig. 3 Plaque morphology of parent WSN and mutant WSN-E190K(HA) viruses on MDCK and NA-MDCK cells. Both viruses were generated by using reverse genetics

Growth properties of the HA mutant

To test the growth properties of the mutant in detail, we first compared the plaque phenotype of the reverse-

genetics-generated parent WSN (WSN-RG) virus with the plaque phenotypes of the mutant viruses (Fig. 3). We confirmed that the WSN-RG virus formed large plaques on MDCK cells and pinpoint plaques on NA-MDCK cells, whereas WSN E190K(HA) virus formed large plaques on NA-MDCK cells. Interestingly, this mutant also formed large plaques on MDCK cells, but their sizes were significantly smaller ($P < 0.05$, Student t-test) than those on NA-MDCK cells. In addition, the plaque sizes of the mutant on NA-MDCK cells were significantly smaller ($P < 0.05$) than those of WSN-RG virus on MDCK cells.

To determine whether the plaque phenotypes correlated with the growth efficiencies of these two viruses, we infected MDCK cells with the viruses at an identical MOI of 0.01 and compared the growth kinetics of the parent and mutant viruses. We found that the growth rate of the mutant was lower than that of the parent WSN (Fig. 4), indicating a positive correlation between plaque phenotype and growth on MDCK cells. On the other hand, although the mutant tended to grow better than the parent virus, the difference in growth rates between the mutant and parent viruses on NA-MDCK cells was not large. This finding is in contrast to that of the plaque sizes of the two viruses, suggesting that, unlike MDCK cells, there is no correlation between the plaque phenotype and growth rate on NA-MDCK cells. Heterogeneous receptor distribution on NA-MDCK cells may be responsible for this discrepancy.

Receptor specificity of the HA mutant

To determine whether the differences in growth properties observed between the parent and mutant viruses are responsible for changes in receptor specificity, we measured the receptor specificity of both viruses by means of a receptor assay using sialylglycopolymers. Interestingly, both viruses had the same receptor specificities; they both recognized both SAα2,3Gal and SAα2,6Gal (Fig. 5).

Since this receptor assay is not quantitative, we next used virus elution from erythrocytes as an assay to compare the receptor binding affinities of the two viruses. The elution assay provides a quantitative assessment of virus binding and release. When we used chicken erythrocytes, the mutant virus was not easily eluted, unlike the parent virus, which was easily eluted for up to 5 h after the temperature shift. By contrast, with guinea pig erythrocytes, we did not observe a marked difference in the elution kinetics between the mutant and parent viruses (Fig. 6). Previous studies [7, 12] as well as our own unpublished observations have shown that chicken and guinea pig erythrocytes contain both SAα2,3Gal and SAα2,6Gal, but quantitative differences between these sialic acids in these species have not been defined. Nonetheless, these data, together with those from the virus elution assay, strongly suggest that the mutant and parent viruses differ in their receptor-binding affinities.

Pathogenicity of the mutant virus in mice

Our *in vitro* assays demonstrated that the HA-NA functional balance of the mutant differs from that of the parent virus. We then asked whether this alteration affects virus pathogenicity in mice. We infected mice with various dilutions of virus and determined the median mouse lethal dose (MLD_{50}), and the results indicated that the mutant was attenuated in these animals ($10^{5.25}$ PFU for WSN-RG vs. $>10^{6.5}$ PFU for WSN-E190K(HA)). To confirm the attenuation phenotype of the mutant, we compared virus titers in organs following intranasal infection with the same amount of the two viruses. We observed no differences in the virus titers in the nasal turbinates but observed significant ($P < 0.05$) differences in the virus titers in the lungs (Fig. 7), indicating that the mutant virus was attenuated in mice and that its pathogenicity may be determined by its growth rate in the lung.

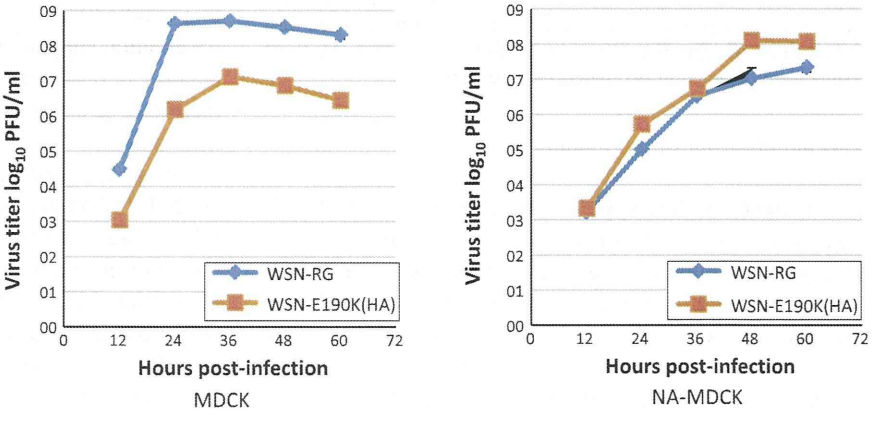

Fig. 4 Growth kinetics of parent WSN and mutant WSN-E190K(HA) viruses on MDCK and NA-MDCK cells. Following infection of cells with each virus at an MOI of 0.01, virus titers were determined by plaque titration with MDCK cells. Experiments were performed three times independently

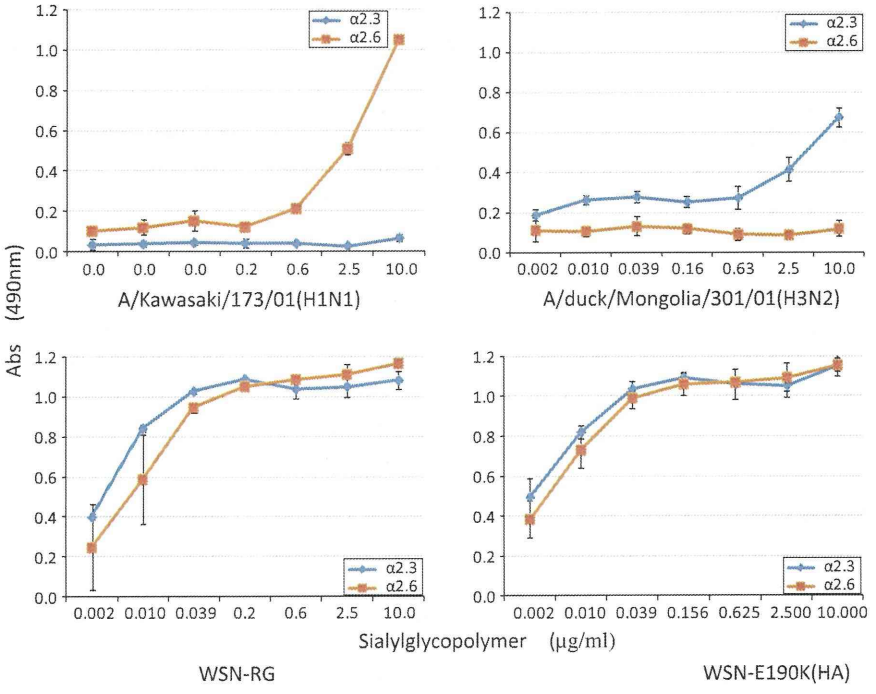

Fig. 5 Receptor binding assay of parent WSN and mutant WSN-E190K(HA) viruses. Each virus was purified through a 25 % sucrose cushion from the supernatant of the infected cell culture and used for the assay. A/Kawasaki/173/01(H1N1) and A/duck/Mongolia/301/01(H3N2) served as controls because they specifically recognize SAα2,6- and SAα2,3-linked receptors, respectively. Experiments were performed three times independently

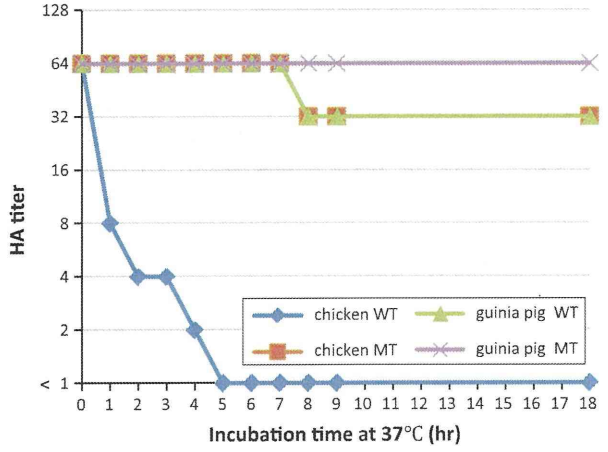

Fig. 6 Virus elution assay using chicken and guinea pig erythrocytes for parent WSN (WT) and mutant WSN-E190K(HA) (MT) virus, respectively. Virus preparations with identical HA titers (64) were incubated with erythrocytes at 4 °C for 1 h, and the plates were then shifted to 37 °C. The HA titers were recorded up to 18 h. Identical results were obtained in two independent experiments

Vaccine potential of the mutant virus

The attenuation phenotype of this mutant suggests that it may have potential as a live vaccine. To assess this possibility, we inoculated mice with a series of dilutions of the mutant virus and then challenged them with 100 MLD_{50} of wild-type WSN at 3 weeks post-immunization. The mice were observed for lethality for 2 weeks. None of the immunized mice died during this observation period, although the body weights of the mice immunized with low titers decrease following challenge with wild-type virus (Fig. 8a). When we attempted to isolate viruses from mouse organs at 3 days post-challenge, no virus was detected from mutant-immunized mice, unlike mock-immunized control mice (Fig. 8b). These data indicate that the mutant virus has potential as a live vaccine against the wild-type virus.

Discussion

In this study, we selected a plaque variant virus, WSN-LPv, derived from the laboratory H1N1 influenza virus, by using NA-expressing MDCK cells. We found that this variant was attenuated in mice when compared with the parent virus, due to an alteration in its HA-NA functional balance that resulted from a single mutation (E190K) in HA. This observation supports the notion that the HA-NA functional balance is responsible for efficient virus growth and can, therefore, be a determinant factor for virus pathogenicity in host animals.

To our knowledge, the HA E190K mutation observed in WSN-LPv has not been found in any naturally occurring H1N1 viruses, although it is well documented that the nature of the amino acid at position 190, in addition to that at position 225, of the HA receptor-binding pocket determines the receptor specificity of H1 viruses [11]. Indeed, Asp (D) at positions 190 and 225 (found in human viruses) confers binding to SAα2,6Gal oligosaccharides, whereas D

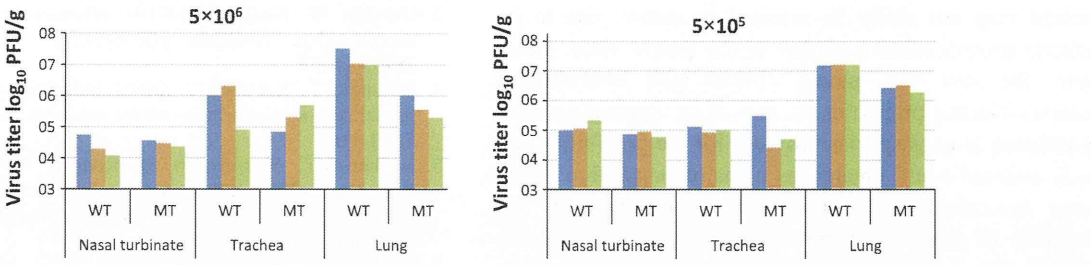

Fig. 7 Virus growth in the organs of mice infected with parent WSN (WT) and mutant WSN-E190K(HA) (MT) viruses. Mice were infected intranasally with two different concentrations of the viruses (5×10^6 or 5×10^5 PFU), and respiratory organs were collected at 3 days post-infection. Virus titers in each organ were determined by plaque titration. Each *bar* indicates the result from one infected mouse

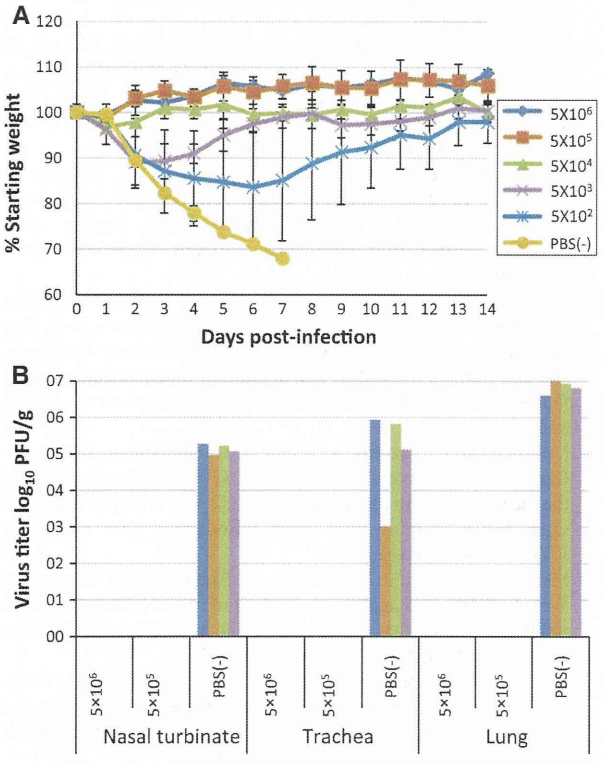

Fig. 8 Protective effects of mutant WSN-E190K(HA) virus against wild-type WSN virus challenge. **a** Mice were immunized intranasally with the indicated titers of mutant virus and were then infected with 100 MLD_{50} of wild-type WSN-RG at 3 weeks post-immunization. Body weights of mice (n = 4/group) were monitored for 14 days. **b** At 3 days post-challenge, four mice in each group were sacrificed for titration of virus present in their organs. Each *bar* indicates the result from one infected mouse. Mock-immunized mice (PBS) were also challenged and examined as controls

and Gly (G) at these positions (found in swine viruses) allow binding to both α2,6 and α2,3 linkages; Glu (E) and G at positions 190 and 225, respectively, (found in avian viruses) permit binding to α2,3-linked sialic acids. Interestingly, WSN-LPv possesses K and D at positions 190 and 225, respectively, whereas the parent WSN virus and even its original human isolate (WS virus; GenBank accession no. CY009604) possess E and D at these positions, which is an unusual combination of amino acids among natural H1N1 viruses. The WSN virus was obtained experimentally through successive passages of the WS virus in ferrets, mice and cell culture and has been maintained by further passages in various laboratories [2, 16]. We do not know the passage history of the WS virus that was used for the database assignment. Nonetheless, these findings support the notion that the amino acids at positions 190 and 225 are "hot spots" for HA mutation in H1N1 viruses that may determine organ tropism as well as host specificity of the virus by altering HA receptor-binding properties.

WSN-LPv with the HA E190K mutation was successfully selected by using our established NA-MDCK cells. Interestingly, SAα2,6Gal, but not SAα2,3Gal, levels were reduced on the surface of NA-MDCK cells when compared with MDCK parent cells. This observation stands in contrast to a previous report describing the preferential substrate specificity of H1N1 virus NAs for SAα2,3Gal over SAα2,6Gal [14]. We do not know the reason for this discrepancy because there is no information about the substrate specificity of WSN NA when expressed on the cell surface. One possible explanation is that a low level of NA expression on NA-MDCK cells may result in different substrate specificity from that measured with other assays in previous studies.

We demonstrated that the HA-NA functional balance of WSN-LPv was altered relative to that of the parent virus, although the receptor specificity of the viruses was not changed. The virus elution assay indicated slower elution from erythrocytes of the variant than of the parent viruses, indicating that the variant had a higher affinity for the receptor molecules. This observation may explain why the variant can replicate efficiently and form large plaques on NA-MDCK cells that have fewer receptor molecules with SAα2,6Gal.

Here, we selected an HA variant with altered receptor-binding activity by using NA-MDCK cells. This kind of

variant may not easily be selected in nature, due to its inferior growth relative to that of the parent virus. However, the idea that mutant viruses with heterologous receptor-binding properties are part of the circulating virus population as quasispecies provides for the possibility that such mutants could emerge as a major population under some biological circumstance, as exemplified by the isolation of 2009 pandemic virus mutants with an HA D225G (H1 numbering: D222G) mutation that are more pathogenic than the original pandemic strain and have enhanced binding to SAα2,3Gal avian-type receptors [1, 10]. Additionally, accidental infection of other animal hosts may lead to the emergence of HA receptor mutants with pandemic potential. Indeed, previous pandemics suggest that pigs are the likely intermediate host animal in which HA receptor mutants are generated [4].

Attenuation of the variant in mice suggests that the HA-NA functional balance of the parent virus was superior to that of the variant for efficient virus replication in lungs, but not in nasal turbinates of mice, revealing that the organ specificity of the virus could be affected by the altered HA-NA functional balance. This finding supports exploring this variant as a potential live vaccine virus because its replication is substantially hampered in the lower respiratory tract. However, attenuation of the variant through an HA single mutation may lead to considerable potential for reversion. Therefore, artificial HA mutations with enhanced receptor-binding affinity should be included in one of the genetic loci for the attenuation phenotype, in addition to cold adaptation with current live vaccines [9], which in turn could lead to the construction of safe live vaccines with high attenuation phenotypes and reduced potential for reversion.

Acknowledgments We thank Dr. Emi Takashita and Susan Watson for providing anti-NA antibody and editing the manuscript. This work was supported by grants-in-aid for Specially Promoted Research and for Scientific Research (B), from the Ministry of Education, Culture, Sports, Science, and Technology, by grants-in-aid from the Ministry of Health, Labor and Welfare, by ERATO, and by National Institute of Allergy and Infectious Diseases Public Health Service research grants.

Conflict of interest The authors declare that they have no conflicts of interest

References

1. Chen H, Wen X, To KK, Wang P, Tse H, chan JF, Tsoi HW, Fung KS, Tse CW, Lee RA, Chan KH, Yuen KY (2010) Quasispecies of the D225G substitution in the hemagglutinin of pandemic influenza A(H1N1) 2009 virus from patients with severe disease in Hong Kong, China. J Infect Dis 201:1517–1521
2. Francis T, Moore AL (1940) A study of the neurotropic tendency in strains of the virus of epidemic influenza. J Exp Med 72: 717–728
3. Gamblin SJ, Skehel JJ (2010) Influenza hemagglutinin and neuraminidase membrane glycoproteins. J Biol Chem 285: 28403–28409
4. Horimoto T, Kawaoka Y (2005) Influenza lessons from past pandemics, warnings from current incidents. Nat Rev Microbiol 3:591–600
5. Hughes MT, Matrosovich M, Rodgers ME, McGregor M, Kawaoka Y (2000) Influenza A viruses lacking sialidase activity can undergo multiple cycles of replication in cell culture, eggs, or mice. J Virol 74:5206–5212
6. Hughes MT, McGregor M, Suzuki T, Suzuki Y, Kawaoka Y (2001) Adaptation of influenza A viruses to cells expressing low levels of sialic acid leads to loss of neuraminidase activity. J Virol 75:3766–3770
7. Ito T, Suzuki Y, Mitnaul L, Vines A, Kida H, Kawaoka Y (1997) Receptor specificity of influenza A viruses correlates with the agglutinin of erythrocytes from different animal species. Virology 227:493–499
8. Ito T, Suzuki Y, Takada A, Kawamoto K, Otsuki K, Masuda H, Yamada M, Suzuki T, Kida H, Kawaoka Y (1997) Differences in sialic acid-galactose linkages in the chicken egg amnion and allantois influence human influenza virus receptor specificity and variant selection. J Virol 71:3357–3362
9. Jin H, Lu B, Zhou H, Ma C, Zhao J, Yang CF, Kemble G, Greenberg H (2003) Multiple amino acid residues confer temperature sensitivity to human influenza virus vaccine strain (FluMist) derived from cold-adapted A/Ann Arbor/6/60. Virology 306:18–24
10. Liu Y, Childs RA, Matrosovich T, Wharton S, Palma AS, Chai W, Daniels R, Gregory V, Uhlendorff J, Kiso M, Klenk H-D, Hay A, Feizi T, Matrosovich M (2010) Altered receptor specificity and cell tropism of D222G hemagglutinin mutants isolated from fatal cases of pandemic A(H1N1) 2009 influenza virus. J Virol 84:12069–12074
11. Matrosovich M, Tuzikov A, Bovin N, Gambaryan A, Klimov A, Castrucci MR, Donatelli I, Kawaoka Y (2000) Early alterations of the receptor-binding properties of H1, H2, and H3 avian influenza virus hemagglutinins after their introduction into mammals. J Virol 74:8502–8512
12. Medeiros R, Escriou N, Naffakh N, Manuguerra J-C, van der Werf S (2001) Hemagglutinin residues of recent human A(H3N2) influenza viruses that contribute to the inability to agglutinate chicken erythrocytes. Virology 289:74–85
13. Mitnaul LJ, Matrosovich M, Castrucci MR, Tuzikov AB, Bovin NV, Kobasa D, Kawaoka Y (2000) Balanced hemagglutinin and neuraminidase activities are critical for efficient replication of influenza A virus. J Virol 74:6015–6020
14. Mochalova L, Kurova V, Shtyrya Y, Korchagina E, Gambaryan A, Belyanchikov I, Bovin N (2007) Oligosaccharide specificity of influenza H1N1 virus neuraminidases. Arch Virol 152: 2047–2057
15. Neumann G, Watanabe T, Ito H, Watanabe S, Goto H, Gao P, Hughes MT, Perez DR, Donis R, Hoffmann E, Hobom G, Kawaoka Y (1999) Generation of influenza A viruses entirely from cloned cDNAs. Proc Natl Acad Sci USA 96:9345–9350
16. Smith W, Andrews CH, Laidlaw PP (1933) A virus obtained from influenza patients. Lancet 2:66–68
17. Totani K, Kubota T, Kuroda T, Murata T, Hidari KI, Suzuki T, Suzuki Y, Kobayashi K, Ashida H, Yamamoto K, Usui T (2003) Chemoenzymatic synthesis and application of glycopolymers containing multivalent sialyloligosaccharides with a poly(L-glutamic acid) backbone for inhibition of infection by influenza viruses. Glycobiology 13:315–326
18. Wagner R, Matrosovich M, Klenk H-D (2002) Functional balance between haemagglutinin and neuraminidase in influenza virus infections. Rev Med Virol 1:159–166

19. Wagner R, Wolff T, Herwig A, Pleschka S, Klenk H-D (2000) Interdependence of hemagglutinin glycosylation and neuraminidase as regulators of influenza virus growth: a study by reverse genetics. J Virol 74:6316–6323
20. Yen HL, Liang CH, Wu CY, Forrest HL, Ferguson A, Choy KT, Jones J, Wong DD, Cheung PP, Hsu CH, Li OT, Yuen KM, Chan RW, Poon LL, Chan MC, Nicholls JM, Krauss S, Wong CH, Guan Y, Webster RG, Webby RJ, Peiris M (2011) Hemagglutinin-neuraminidase balance confers respiratory-droplet transmissibility of the pandemic H1N1 influenza virus in ferrets. Proc Natl Acad Sci USA 108:14264–14269

ヘパリンによる侵入阻害作用に基づく抗原虫薬およびワクチン開発へのアプローチ

小林　郷介[1,2]、竹前　　等[1]、杉　　達紀[1]、龔　　海燕[1]、F. レクエンコ[1]
岩永　達也[1]、堀本　泰介[1]、明石　博臣[1]、加藤健太郎[1]
[1]東京大学大学院農学生命科学研究科獣医微生物学研究室
[2]東京大学医科学研究所付属幹細胞治療研究センター幹細胞プロセシング分野

Approach for the development of antiprotozoal agents and vaccines on the basis of invasion inhibitory effect of heparin

Kyousuke Kobayashi[1,2], Hitoshi Takemae[1], Tatsuki Sugi[1], Haiyan Gong[1], Recuenco C. Frances[1]
Tatsuya Iwanaga[1], Taisuke Horimoto[1], Hiroomi Akashi[1], Kentaro Kato[1]
[1]Department of Veterinary Microbiology, Graduate School of Agricultural and Life Sciences, University of Tokyo
[2]Division of Stem Cell Processing, Center for Stem Cell Biology and Regenerative Medicine, Institute of Medical Science, University of Tokyo

我々は、原虫独特の生活環を遮断する新たな薬剤やワクチンのターゲットとして「宿主細胞侵入」に注目して研究を行っている。中でもヒトに深刻な健康危害をもたらす熱帯熱マラリア原虫は、細胞侵入機構の研究において優れたモデルといえる。我々が着目する「ヘパリン」が、マラリア原虫に対して増殖阻害活性を示すことは過去にも報告があるが、阻害のメカニズムは明らかではない。そこで我々は、ヘパリンによる細胞侵入阻害機序の解明を試みた。

解析の結果、いくつかの侵入阻害モデルが浮かび上がってきた。ひとつは、侵入を媒介する複数のレセプター・リガンド結合が同時に阻害される可能性。あるいは、メロゾイト先端部がヘパリンで覆われることで赤血球表面との接近が物理的に障害される可能性である（図1）。

我々は、この結果を薬剤やワクチンの開発に応用することを目指したアプローチとして以下の二点を現在検討している。(1) ヘパリンが阻害活性を示す上で重要となる構造を特定することで、実用的な薬剤が開発できるか。(2) 分離したヘパリン結合タンパク質を有効なワクチン抗原として用いることができるか。

マラリア原虫以外にもヘパリンによる細胞侵入阻害を示す原虫が報告されているため、本研究で得られた知見は、抗原虫感染症戦略における一つのモデルとなることが期待できる。

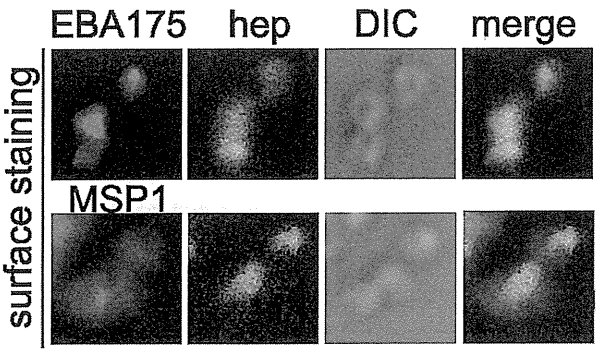

図1．メロゾイト表面におけるビオチン標識ヘパリンの結合部位

Key words：malaria, merozoite, invasion, heparin

引用文献

Boyle, M. J. *et al.* 2010. Interactions with heparin-like molecules during erythrocyte invasion by *Plasmodium falciparum*. merozoites. *Blood* 115：4559-4568.

Kobayashi, K. *et al.* 2010. *Plasmodium falciparum* BAEBL binds to heparan sulfate proteoglycans on the human erythrocyte surface. *J. Biol. Chem.* 285：1716-1725.

連絡先責任者：加藤健太郎、東京大学大学院農学生命科学研究科獣医微生物学研究室、〒113-8657　東京都文京区弥生 1-1-1、E-mail：akkato@mail.ecc.u-tokyo.ac.jp
Correspondence：K. Kato, Department of Veterinary Microbiology, Graduate School of Agricultural and Life Sciences, University of Tokyo, 1-1-1 Yayoi, Bunkyo-ku, Tokyo 113-8657

Parasitology International 61 (2012) 224–234

Contents lists available at SciVerse ScienceDirect

Parasitology International

journal homepage: www.elsevier.com/locate/parint

Review

Roles of Apicomplexan protein kinases at each life cycle stage

Kentaro Kato *, Tatsuki Sugi, Tatsuya Iwanaga

Department of Veterinary Microbiology, Graduate School of Agricultural and Life Sciences, The University of Tokyo, 1-1-1 Yayoi, Bunkyo-ku, Tokyo 113-8657, Japan

ARTICLE INFO

Article history:
Received 18 August 2011
Received in revised form 12 December 2011
Accepted 18 December 2011
Available online 24 December 2011

Keywords:
Apicomplexan protein kinase
Life cycle
Plasmodium
Protein kinase inhibitor
Toxoplasma

ABSTRACT

Inhibitors of cellular protein kinases have been reported to inhibit the development of Apicomplexan parasites, suggesting that the functions of protozoan protein kinases are critical for their life cycle. However, the specific roles of these protein kinases cannot be determined using only these inhibitors without molecular analysis, including gene disruption. In this report, we describe the functions of Apicomplexan protein kinases in each parasite life stage and the potential of pre-existing protein kinase inhibitors as Apicomplexan drugs against, mainly, *Plasmodium* and *Toxoplasma*.

Contents

1. Introduction

Some Apicomplexan parasites are known to be pathogens that cause lethal symptoms, including zoonoses, in humans, warm-blooded animals and insect vectors. Vaccines against the Apicomplexan parasites have not yet been developed. Although anti-protozoan drugs have been used in epidemic countries, drug-resistance frequently occurs. How is the damage caused by Apicomplexan parasites to be overcome?

Apicomplexan parasites, which have common characteristic organelles at the apex in the invasive forms, such as the dense granule, microneme, rhoptry, are the most-studied protozoans. Their life cycles are complex, compared to those of other biological species. Data described below suggest that protein kinases encoded by parasites are the main trigger molecules of life stage conversions. Addition of some protein kinase inhibitors causes specific inhibition of one parasite life cycle event. Phosphorylation by cellular protein kinases has been reported to regulate important cellular processes such as transcription, translation, protein synthesis, cell cycle, and apoptosis. Therefore, the protein kinases encoded by the parasite genomes may represent drug targets to block parasite-specific life events.

* Corresponding author. Tel.: +81 3 5841 5398; fax: +81 3 5841 8184.
E-mail address: akkato@mail.ecc.u-tokyo.ac.jp (K. Kato).

1383-5769/$ – see front matter © 2011 Elsevier Ireland Ltd. All rights reserved.
doi:10.1016/j.parint.2011.12.002

However, the roles of each Apicomplexan protein kinase could not be determined using growth assays with protein kinase inhibitors. In this report, we reviewed the functions of Apicomplexan protein kinases by parasite life stage and the effects of pre-existing protein kinase inhibitors on, mainly, *Plasmodium* and *Toxoplasma*.

2. The functions of *Plasmodium* protein kinases in the life cycle and the effects of protein kinase inhibitors

The life cycle of *Plasmodium* (Fig. 1) is summarized below. Sporozoites are delivered into the bloodstream by the bite of an infected *Anopheles* mosquitoes. The sporozoites invade hepatocytes and produce several thousand merozoites. The merozoite invades erythrocytes and develops into the ring form, trophozoite, schizont. After rupture of the infected erythrocyte, the merozoites in mature schizonts burst out into the bloodstream and invade new erythrocytes, repeating the erythrocytic schizogony. During erythrocytic schizogony, a portion of parasites differentiate into micro- or macrogametocytes. Following the bite, gametogenesis occurs in the blood meal of the mosquito. After fertilization, the zygote is generated and develops into a motile ookinete. The ookinete establishes an oocyst at the basal lamina of the midgut. The oocyst generates sporozoites, which accumulate in the salivary glands.

In the life cycle, *Plasmodium* protein kinases regulate the life stage conversions (Fig. 1). The addition of protein kinase inhibitors causes specific inhibition of each life cycle event of *Plasmodium* although the targets of most of inhibitors are not specific. The method to knock out the specific gene of *Plasmodium* is useful for inhibit the specific protein kinase. However, the parasite in which the essential genes are knocked out for the life cycle event, especially blood stage, could not be produced. The conditional knockout system is not used as a large strategy and is still needed to be improved when used in *Plasmodium* species though one report showed successful knockdown using the destabilizing domain system [1]. We described the functions of *Plasmodium* protein kinases in the life cycle and the effects of protein kinase inhibitors below. The evaluation of effects of these pre-existing protein kinase inhibitors on *Plasmodium* is summarized in Table 1.

2.1. Invasion and egress

Protein kinases expressed in the invasive forms of parasites can play a role in the invasion step. *P. falciparum* protein kinase 2 (PfPK2), which is the only gene homologous to human calcium calmodulin-dependent protein kinase in the *P. falciparum* genome, is expressed in the merozoite [2]. W-7, a calmodulin antagonist,

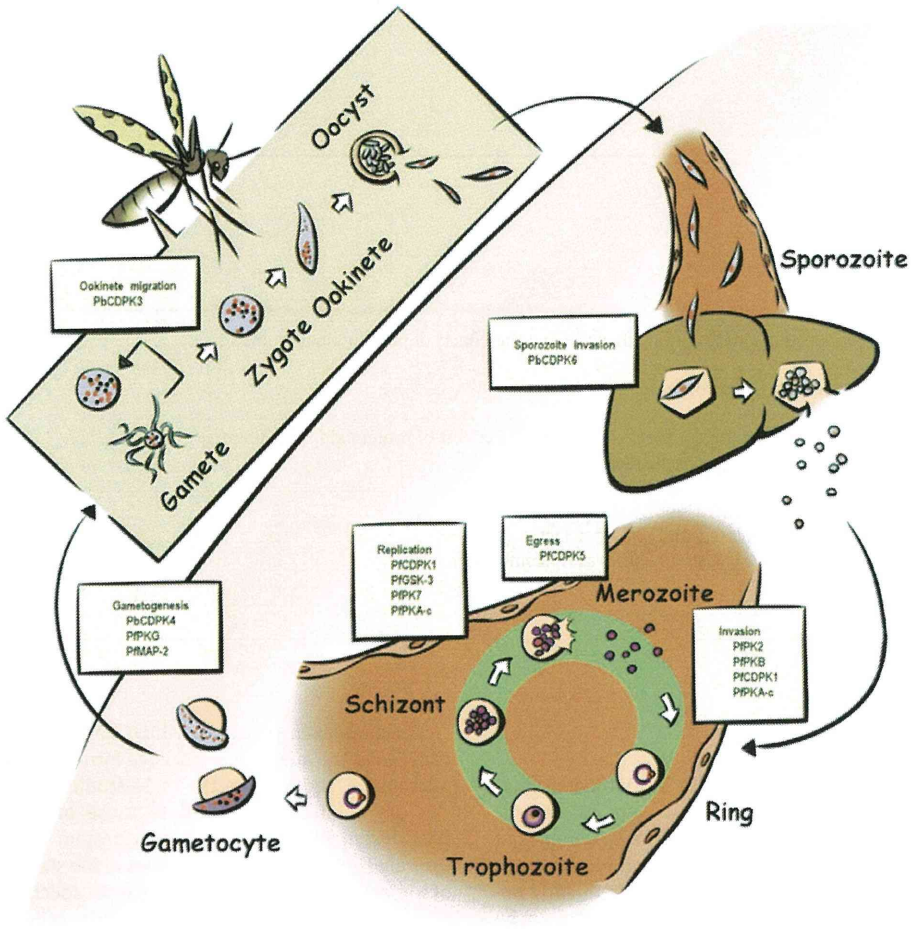

Fig. 1. Functions of *Plasmodium* protein kinases at each stage of the *Plasmodium* life cycle. *Plasmodium falciparum* protein kiase 2 (PfPK2) [2], protein kinase B (PfPKB) [3–6], calcium-dependent protein kinase 1 (PfCDPK1) [7] and PfPKA-C [8] are expressed in merozoites or associated with merozoite invasion. PfCDPK1 [17], glycogen synthase kinase-3 (PfGSK-3) [18] and PfPK7 [23] act on replication in erythrocytes. PfCDPK5 is critical for egress from the infected erythrocyte [1]. *Plasmodium berghei* calcium-dependent protein kinase 4 (PbCDPK4) and cGMP-dependent protein kinase (PfPKG) are essential for the exflagellation of male gametocytes induced by xanthurenic acid (XA) [36]. Mitogen-activated kinase-2 (PfMAP-2) is expressed in gametocytes [40]. PbCDPK3 regulates ookinete gliding mobility and penetration into the layer covering the midgut epithelium [14,15]. PbCDPK6 is critical for the switch to a hepatocyte-invasive phenotype [16].

Table 1
Evaluation of the effects of pre-existing protein kinase inhibitors on *Plasmodium*.

Inhibitor	Kinase family	Species	Strain	IC_{50} (nM)	Procedure						Reference
					Test	Parasitemia (%)	Hematocrit (%)	Starting stage	Incubation	Method	
Compound 1	PKG	Pf	3D7	<1000	Invasion	0.5	1	Schizont	24 h	Microscopy	11
				No effect in 1000	Grow (ring to troph)	0.5	1	Ring	24 h		
		Pf	3D7	2700	Growth	?	?	Early trophzoite	24 h	[^{3}H]-hypoxanthine uptake	25
				<300	Gametogenesis (rounding-up)	?	?	Gametocytes	10 min with XA and drug	Microscopy	
				<6000	Gametogenesis (exflagellation)						
		Pf	NF54	490	Growth	0.5	2.5	Early ring	48 h	[^{3}H]-hypoxanthine uptake	12
			Dd2	1300							
		Pb	?	Delayed mice mortality in 50 mg/kg	Growth	–	–	–	–	Virulence	
H89	PKA	Pf	D6	2900	Growth	0.1–0.5	1.5	?	42 h	[^{3}H]-hypoxanthine uptake	21
			W2	2500							
		Pb	234L clone	Reduced in 50,000	Gametologenesis (exflagellation)	?	10	Gametocytes	15 min	Microscopy	42
K252a	CDPK	Pf	3D7	348	Growth	0.5	2	Late stage schizont	48 h	Microscopy	7
KN-93	CaMK	Pg	8A	700	Zygotes to ookinetes	?	?	Zygotes	Overnight	Microscopy	41
W-7 (CAM antagonist)	CaMK	Pf	3D7	Reduced in 50,000	Invasion	?	?	Schizont	24 h	Microscopy	2
Go 6983	PKC	Pf	3D7	Reduced in 5000	Growth (schizont to ring)	1	?	Ring>80%	10–48 h	Microscopy	4
				Reduced in 2000, 5000	Invasion	?	?	Schizont	2–8 h	Microscopy	
U0126	MAPK	Pf	3D7	3000	Growth	0.5	5	Asynchronized	24 + 24 h with [^{3}H]-hypoxanthine	[^{3}H]-hypoxanthine uptake	27
PD98059				30,000							
PD184352				7000							
Alsterpaullone	CDK	Pf	W2	4300	Growth	3	?	Ring>70%	24 + 18 h with [^{3}H]-hypoxanthine	[^{3}H]-hypoxanthine uptake	29
			D6	4300							
		Pf	W2	4300							33
Butyrolactone 1		Pf	W2	11,700							29
			D6	11,700							
Indirubin-3′-monoxine			W2	1100							
			D6	600							
Indirubin		Pf	W2	1100							33
Isopentenyladenine		Pf	FCR-3	8340	Growth	0.5	1	Ring	24 h + 52 h with [^{3}H]-hypoxanthine	[^{3}H]-hypoxanthine uptake	31
Kenpaullone		Pf	W2	3800	Growth	3	?	Ring>70%	24 h + 18 h with [^{3}H]-hypoxanthine	[^{3}H]-hypoxanthine uptake	29
			D6	3800							
Olomoucine			W2	8000							
			D6	2700							
		Pf	K1	15,000	Growth	0.8	1.0	Ring	48 h with [^{3}H]-hypoxanthine	[^{3}H]-hypoxanthine uptake	32
		Pf	FCR-3	8450	Growth	0.5	1	Ring	24 h + 52 h with [^{3}H]-hypoxanthine	[^{3}H]-hypoxanthine uptake	31
Roscovitine		Pf	W2	28,000	Growth	3	?	Ring>70%	24 h + 18 h with [^{3}H]-hypoxanthine	[^{3}H]-hypoxanthine uptake	29
			D6	33,000							
		Pf	FCR-3	5350	Growth	0.5	1	Ring	24 h + 52 h with [^{3}H]-hypoxanthine	[^{3}H]-hypothxanthine uptake	31
Purvalanol A		Pf	W2	9200	Growth	3	?	Ring>70%	24 h + 18 h with [^{3}H]-hypoxanthine	[^{3}H]-hypoxanthine uptake	29
			D6	2600							
Purvalanol A (S-isomer)		Pf	FCR-3	420	Growth	0.5	1	Ring	24 h + 52 h with [^{3}H]-hypoxanthine	[^{3}H]-hypoxanthine uptake	31
Purvalanol A (R-isomer)				550							
Purvalanol B				7070							

Table 1 (*continued*)

Inhibitor	Kinase family	Species	Strain	IC_{50} (nM)	Procedure						Reference
					Test	Parasitemia (%)	Hematocrit (%)	Starting stage	Incubation	Method	
Methyl-purvalanol B				47,450							
Aminopurvalanol				11,040							
Flavopiridol		Pf	K1	2000	Growth	0.8	1.0	Ring	48 h	[^{3}H]-hypoxanthine	32
Staurosporine	Most of kinase	Pk	?	250	Invasion into rhesus monkey RBC	?	?	Merozoite	Preincubation 5 min + invasion 2–3 h	Microscopy	9
		Pf	?	Reduced in 800	Invasion	?	?	Merozoite	20 h	Microscopy	10
		Pf	W2	150	Growth	3	?	Ring>70%	24 h + 18 h with [^{3}H]-hypoxanthine	[^{3}H]-hypoxanthine uptake	29
			D6	190							
K510	Unclear	Pf	3D7	2500	Growth	?	?	?	48 h	[^{3}H]-hypoxanthine uptake	24
K109				1000							
K497				1500							
Xestoquione	Unclear	Pf	FCB1	3000	Growth	1	1.5	Mostly at ring	48 h	LDH activity	26
Oxindole-based inhibitor 14	CDK	Pf	W2	>20	Growth	3	?	Ring>70%	24 h + 18 h with [^{3}H]-hypoxanthine	[^{3}H]-hypoxanthine uptake	29
			D6	>20							
Oxindole-based inhibitor 15			W2	>15.2							
			D6	>15.2							
Oxindole-based inhibitor 16			W2	>14.6							
			D6	>14.6							
Oxindole-based inhibitor 17			W2	>15.2							
			D6	>15.2							
Oxindole-based inhibitor 18			W2	>14.4							
			D6	>14.4							
Purine-derivative compound 99	CDK	Pf	FCR-3	830	Growth	0.5	1	Ring	24 h + 52 h with [^{3}H]-hypoxanthine	[^{3}H]-hypoxanthine uptake	31
Purine-derivative compound 101				630							
Purine-derivative compound 40				540							
Purine-derivative compound 43				1120							
Purine-derivative compound 52				7100							
Purine-derivative compound 51				560							
Purine-derivative compound 52M				32,300							
Purine-derivative compound 59				530							
Purine-derivative compound 66				No inhibition at 10,000							
Sulfonamide-derivative compound 6	CDK	Pf	W2	17,000	Growth	3	?	Ring>70%	24 h + 18 h with [^{3}H]-hypoxanthine	[^{3}H]-hypoxanthine uptake	33
Sulfonamide-derivative compound 11				31,700							
Sulfonamide-derivative compound 12				24,700							
Sulfonamide-derivative compound 16				31,000							
Sulfonamide-derivative compound 20				21,200							
Sulfonamide-derivative compound 26				23,300							
Benzamides	Unclear	Pf	3D7, etc.	44–8000	Growth?	?	?	?	?	?	35
Imidazopyridazine compounds (Compound 2)	Unclear	Pf	?	5700	Growth?	?	?	?	?	?	34

–, needless to be described; ?, no description; Pf, *Plasmodium falciparum*; Pb, *Plasmodium berghei*; Pk, *Plasmodium knowlesi*; PKG, cGMP-dependent protein kinase; PKA, cAMP-dependent protein kinase; CDPK, calcium-dependent protein kinase; CaMK, calcium/calmodulin-dependent kinase; PKC, protein kinase C; MAPK, mitogen-activated protein kinase; CDK, cyclin-dependent protein kinase; XA, xanthurenic acid; LDH, lactate dehydrogenase.